MIMO-OFDM Systems in the Presence of Phase Noise and Doubly Selective Fading

Yu Zhang, *Student Member, IEEE*, and Huaping Liu, *Member, IEEE*

***Abstract*—In this paper, we analyze the effects of phase noise to multiple-input multiple-output (MIMO) orthogonal frequency division multiplexing (OFDM) systems over doubly selective Rayleigh fading channels. Similar to single-antenna OFDM, MIMO-OFDM suffers from significant performance degradation due to phase noise and time-selective fading, which causes intercarrier interference (ICI). We derive the expressions of carrier-to-interference and signal-to-interference-plus-noise ratios. After characterizing the common phase error (CPE) caused by phase noise and ICI caused by phase noise, as well as time-selective fading, we then derive a minimum mean-squared error-based scheme to mitigate the effect of both phase noise and time-selective fading. We also evaluate and compare the performances of various detection schemes combined with the proposed CPE mitigation scheme. Through numerical results, we examine the relative performances and the potential error floors of these detection schemes.**

***Index Terms*—Intercarrier interference (ICI), orthogonal frequency division multiplexing (OFDM), phase noise, time-selective fading.**

I. Introduction

ORTHOGONAL frequency division multiplexing (OFDM) is considered a promising transmission technique for wideband wireless communications. One of the disadvantages of OFDM is its sensitivity to phase noise, which is a random process caused by the fluctuation of the transmitter and receiver oscillators [1]. It is widely accepted that phase noise in OFDM has two major effects [2], [3]: common phase error (CPE), a constant rotation to the signal constellation, and intercarrier interference (ICI) due to the loss of orthogonality among subcarriers caused by the fast changes of the oscillator phase. The CPE term is the same for all subcarriers within one OFDM symbol interval and changes slowly from one symbol to another. If phase noise level is low, CPE approximately equals the mean of the phase deviation of an oscillator within one OFDM symbol. The ICI term is a random process. Schemes which compensate phase noise in OFDM systems have been proposed in [4] and [5]. In [6], the signal-to-interference-plus-noise ratio (SINR) expression for single-antenna OFDM systems with various phase-noise levels and different number of subcarriers was derived.

Manuscript received December 28, 2005; revised June 29, 2006 and August 21, 2006. The review of this paper was coordinated by Dr. E. Larsson.

The authors are with the School of Electrical Engineering and Computer Science, Oregon State University, Corvallis, OR 97331 USA (e-mail: zhangyu@eecs.oregonstate.edu; hliu@eecs.oregonstate.edu).

Color versions of one or more of the figures in this paper are available online at http://ieeexplore.ieee.org.

Digital Object Identifier 10.1109/TVT.2007.897236

Multiple-input multiple-output (MIMO) antennas have been combined with OFDM to improve spectral efficiency through spatial multiplexing [7]. Similar to single-antenna OFDM, MIMO-OFDM is also highly sensitive to phase noise. CPE estimation schemes for MIMO-OFDM systems were derived in [8] and [9], a decision-directed approach for compensation of phase noise in MIMO-OFDM systems was studied. Besides phase noise, time-selective fading also destroys the orthogonality among different subcarriers within one OFDM symbol and causes ICI [10], [11]. Similar to single-antenna OFDM, MIMO-OFDM is also vulnerable to channel time selectivity. Error performance of MIMO-OFDM systems in the presence of time-selective fading without considering phase noise was analyzed in [12].

Although the issue caused by phase noise and time-selective fading in MIMO-OFDM has been recognized, the exact quantitative effect of the combination of the two has not been well addressed. Phase-noise mitigation for MIMO-OFDM in fast time-varying fading environments has not been well studied either. In this paper, we analyze, via mainly an analytical approach, the impact of phase noise to the performance of MIMO-OFDM systems over doubly selective (channel is both time-selective and frequency-selective) Rayleigh fading channels. After characterizing CPE caused by phase noise and ICI caused by phase noise and time-selective fading, we derive a minimum mean square error (mmse)-based mitigation scheme to effectively minimize the impact of phase noise. We also compare four detection schemes—the zero-forcing (ZF) scheme [13], the mmse scheme [14], the decorrelating decision-feedback (DF) scheme [15], and the mmse-DF scheme [16], [17]—and evaluate their symbol-error-rate (SER) performance. This paper is organized as follows. Section II provides the MIMO-OFDM system model. Analysis of the impact of phase noise and time-selective fading is described in detail in Section III. The mmse-based phase noise suppression approach and various detection schemes are studied in Section IV. Simulation results are given in Section V, followed by concluding remarks in Section VI.

II. System Model

The following notation will be used in this paper. Column vectors/matrices are denoted by boldface lower/upper case letters; superscripts $(\cdot)^{\mathrm{T}}$, $(\cdot)^*$, $(\cdot)^{\mathrm{H}}$, and $(\cdot)^\dagger$ denote transpose, complex conjugate, complex conjugate transpose and pseudoinverse, respectively; $E[\cdot]$, $\mathrm{var}(\cdot)$, and $\mathrm{cov}(\cdot)$ stand for expectation, variance, and covariance, respectively; $\boldsymbol{I}_N$ represents the $N \times N$ identity matrix; $\otimes$ denotes Kronecker product; $\|\cdot\|_F$

denotes the Frobenius norm; $\mathrm{tr}(\cdot)$ denotes the trace of a matrix; $\{\boldsymbol{A}\}_{ij}$ denotes the (i,j)th element of matrix $\boldsymbol{A}$.

Consider a MIMO-OFDM system with N_t transmit antennas, N_r receive antennas, and N_s subcarriers in a doubly selective Rayleigh fading environment. Input data are assumed to be independent variables with zero mean and unit variance. The time domain data sequence is obtained by taking the inverse discrete Fourier transform (DFT) of the data block for each transmit antenna. A cyclic prefix (CP) with a length longer than the channel length is inserted at the beginning of each of the data sequences. The data sequences with a CP are then transmitted through N_t independent antennas. At each receive antenna, the CP is removed and a DFT unit is applied. Let $\boldsymbol{x}_k = [x_{k1}, \ldots, x_{kN_\mathrm{t}}]^\mathrm{T}$ and $\boldsymbol{y}_k = [y_{k1}, \ldots, y_{kN_\mathrm{r}}]^\mathrm{T}$ denote, respectively, the transmitted and received data for all antennas on subcarrier k, where $0 \le k \le N_\mathrm{s} - 1$. The general form of the received signal in MIMO-OFDM over slowly fading channels (the channel is time-invariant over several OFDM symbol periods) is expressed as

$$\boldsymbol{y}_k = \Delta_k \boldsymbol{x}_k + \boldsymbol{n}_k \tag{1}$$

where Δ_k is an $N_\mathrm{r} \times N_\mathrm{t}$ matrix whose (i,j)th component, $\{\Delta_k\}_{ij}$, denotes the channel frequency response between the jth transmit antenna and the ith receive antenna and $\boldsymbol{n}_k$ is an $N_\mathrm{r} \times 1$ Gaussian noise vector on subcarrier k. Elements of $\boldsymbol{n}_k$ have zero mean and variance σ^2.

Phase noise $\phi(t)$ may be described as a continuous Brownian motion process with zero mean and variance $2\pi\beta t$, where β denotes the two-sided 3-dB linewidth of the Lorentzian power density spectrum of the free-running carrier generator [1]. For the analysis in this paper, we need to consider discretized Brownian motion $\phi(n) = \phi(nT_\mathrm{s})$, where T_s is the data symbol period. Thus, we have $\phi(n+1) = \phi(n) + \varsigma(n)$, where $\varsigma(n) \sim \mathcal{N}(0, 2\pi\beta T_\mathrm{s})$ is a Gaussian random variable with zero mean and variance $\sigma_\varsigma^2 = 2\pi\beta T_\mathrm{s}$. If we assume that only one oscillator is used to support multiple antennas, (1) needs to be modified to take into account the effects of phase noise as [6]

$$\boldsymbol{y}_k = \Delta_k \boldsymbol{x}_k I(0) + \sum_{\substack{k'=0 \\ k' \ne k}}^{N_\mathrm{s}-1} \Delta_{k'} \boldsymbol{x}_{k'} I(k'-k) + \boldsymbol{n}_k \tag{2}$$

where

$$I(f) = \frac{1}{N_\mathrm{s}} \sum_{n=0}^{N_\mathrm{s}-1} e^{j\frac{2\pi f n}{N_\mathrm{s}} + j\phi(n)}. \tag{3}$$

Note that CPE and ICI due to phase noise are represented by $I(0)$ and the second term on the right-hand side of (2), respectively.

III. Impact of ICI Caused by Phase Noise and Time-Varying Fading

In the presence of phase noise and time-selective fading, the effective $N_\mathrm{s}N_\mathrm{r} \times N_\mathrm{s}N_\mathrm{t}$ spatiotemporal channel matrix $\boldsymbol{H}_\mathrm{t}$ during the tth OFDM symbol period with the effects of phase noise taken into consideration is given by (4), shown at the bottom of the page, as [18], where L is the number of resolvable paths and $\boldsymbol{0}$ is an $N_\mathrm{r} \times N_\mathrm{t}$ zero matrix. Each nonzero block of $\boldsymbol{H}_\mathrm{t}$ contains the $N_\mathrm{r} \times N_\mathrm{t}$ channel matrix $\boldsymbol{H}_{t,l}(n)$ for path l at time nT_s. Note that the index in the parenthesis following $\boldsymbol{H}_{t,l}$ is the time index. For simplicity of notation, we will omit the time index t which represents the OFDM symbol period hereafter.

Assuming a wide sense stationary uncorrelated scattering channel [12], all elements of $\boldsymbol{H}_l(n)$ are modeled as independent complex Gaussian random variables with zero mean and equal variance. The channel is assumed to have an exponential power delay profile $\theta(\tau_l) = e^{-\tau_l/\tau_\mathrm{rms}}$ [19], where τ_l is the delay of the lth path and τ_rms represents the root-mean-square (rms) delay spread. Since the channel is time-variant, the relationship between the channel coefficients for path l at times nT_s and $(n+m)T_\mathrm{s}$ can be described as [20]

$$\{\boldsymbol{H}_l(n+m)\}_{ij} = \alpha_m \{\boldsymbol{H}_l(n)\}_{ij} + \rho_{l,ij}(n+m) \tag{5}$$

where

$$\alpha_m = \frac{E\left[\{\boldsymbol{H}_l(n)\}_{ij} \cdot \{\boldsymbol{H}_l(n+m)\}_{ij}^*\right]}{e^{-\frac{\tau_l}{\tau_\mathrm{rms}}}} = J_0(2\pi m f_\mathrm{d} T_\mathrm{s}) \tag{6}$$

where f_d is the maximum Doppler shift, $J_0(\cdot)$ is the zero-order Bessel function of the first kind, and $\{\rho_{l,ij}(n)\}$ are independent complex Gaussian random variables with zero mean and variance $e^{-\tau_l/\tau_\mathrm{rms}}(1-\alpha_m^2)$.

Had the system been phase-noise free and the channel been time-invariant, $\boldsymbol{H}$ given in (4) would have had the eigendecomposition $\boldsymbol{H} = (\boldsymbol{U} \otimes \boldsymbol{I}_{N_\mathrm{r}})^\mathrm{H} \Lambda (\boldsymbol{U} \otimes \boldsymbol{I}_{N_\mathrm{t}})$, where $\boldsymbol{U}$ is the unitary DFT matrix with $\{\boldsymbol{U}\}_{ij} = 1/\sqrt{N_\mathrm{s}} e^{(-2\pi\sqrt{-1}/N_\mathrm{s})ij}$, $0 \le i, j \le N_\mathrm{s} - 1$, and Λ is a block diagonal matrix whose (k,k)th block equals Δ_k [12]. This establishes the relationship between the channel frequency response given in (1) and (2), and the channel coefficients in the time domain.

$$\boldsymbol{H}_\mathrm{t} = \begin{bmatrix} \boldsymbol{H}_{t,0}(0)e^{j\phi(0)} & \cdots & 0 & \cdots & \boldsymbol{H}_{t,1}(0)e^{j\phi(0)} \\ \vdots & & \vdots & & \vdots \\ \boldsymbol{H}_{t,L-1}(L-1)e^{j\phi(L-1)} & \cdots & \boldsymbol{H}_{t,0}(L-1)e^{j\phi(L-1)} & \cdots & 0 \\ \vdots & & \vdots & & \vdots \\ 0 & \cdots & \boldsymbol{H}_{t,L-1}(N_\mathrm{s}-1)e^{j\phi(N_\mathrm{s}-1)} & \cdots & \boldsymbol{H}_{t,0}(N_\mathrm{s}-1)e^{j\phi(N_\mathrm{s}-1)} \end{bmatrix} \tag{4}$$

With the effective channel matrix given in (4), we let $\boldsymbol{G} = (\boldsymbol{U} \otimes \boldsymbol{I}_{N_\mathrm{r}})\boldsymbol{H}(\boldsymbol{U} \otimes \boldsymbol{I}_{N_\mathrm{t}})^\mathrm{H}$, which is no longer a block diagonal matrix. This shows that phase noise and time-selective fading cause ICI, which is represented by the off-diagonal blocks of $\boldsymbol{G}$. Let $\boldsymbol{G}_{ij}$ denote the (i,j)th block of $\boldsymbol{G}$. The ideal model given in (1) needs to be generalized to reflect the impacts of both time-selective fading and phase noise as

$$\boldsymbol{y}_k = \boldsymbol{G}_{kk}\boldsymbol{x}_k + \sum_{\substack{k'=0 \\ k' \neq k}}^{N_\mathrm{s}-1} \boldsymbol{G}_{kk'}\boldsymbol{x}_{k'} + \boldsymbol{n}_k, \qquad k = 0, \ldots, N_\mathrm{s}-1. \tag{7}$$

Let $\boldsymbol{\Upsilon}p_{ij}$ be an $N_\mathrm{s} \times N_\mathrm{s}$ matrix given by

$$\boldsymbol{\Upsilon}_{ij} = \begin{bmatrix} \mathrm{var}\left(\{\boldsymbol{G}_{00}\}_{ij}\right) & \cdots & \mathrm{var}\left(\{\boldsymbol{G}_{0,N_\mathrm{s}-1}\}_{ij}\right) \\ \vdots & \ddots & \vdots \\ \mathrm{var}\left(\{\boldsymbol{G}_{N_\mathrm{s}-1,0}\}_{ij}\right) & \cdots & \mathrm{var}\left(\{\boldsymbol{G}_{N_\mathrm{s}-1,N_\mathrm{s}-1}\}_{ij}\right) \end{bmatrix}. \tag{8}$$

As shown in Appendix A, $\boldsymbol{\Upsilon}p_{ij}$ has a circulant structure expressed as

$$\boldsymbol{\Upsilon}_{ij} = \begin{bmatrix} \gamma_0 & \gamma_1 & \cdots & \gamma_{N_\mathrm{s}-1} \\ \gamma_{N_\mathrm{s}-1} & \gamma_0 & \cdots & \gamma_{N_\mathrm{s}-2} \\ \vdots & \vdots & & \vdots \\ \gamma_1 & \gamma_2 & \cdots & \gamma_0 \end{bmatrix}, \qquad 1 \le i \le N_\mathrm{r}; \quad 1 \le j \le N_\mathrm{t}\ . \tag{9}$$

Since elements of $\boldsymbol{G}_{ij}$ are independent and identically distributed Gaussian random variables [12], (9) applies to all antennas. It is also shown in Appendix A that γ_k defined in (9) can be expressed in closed-form as

$$\gamma_k = \frac{1}{N_\mathrm{s}^2}\sum_{l=0}^{L-1}\left\{ N_\mathrm{s} + 2\sum_{i=1}^{N_\mathrm{s}-1}(N_\mathrm{s}-i)J_0(2\pi i f_\mathrm{d} T_\mathrm{s}) \times \cos\left(\frac{2\pi}{N_\mathrm{s}}ki\right) e^{-\pi\beta T_\mathrm{s} i}\right\} e^{-\frac{\tau_l}{\tau_\mathrm{rms}}}, \quad k = 0, \ldots, N_\mathrm{s}-1. \tag{10}$$

ICI can be well quantified by using the carrier-to-interference ratio (CIR) [21]. In order to quantify the combined effects of both phase noise and time-selective fading, we derive CIR as a function of the two-sided 3-dB linewidth β, the number of subcarriers, and the normalized Doppler shift ($f_\mathrm{d}T_\mathrm{s}$). In the presence of phase noise and time-selective fading, CIR of the kth subcarrier for MIMO-OFDM systems is given by (11), shown at the bottom of the page. The details of the derivation of (11) are given in Appendix B. Note that CIR is independent of the channel power-delay profile and the number of resolvable paths, and is the same for all subcarriers. Furthermore, the SINR expression of MIMO-OFDM systems in the presence of phase noise and time-selective fading, as described in detail in Appendix B, is given as

$$\mathrm{SINR} = \frac{N_\mathrm{t}\gamma_0}{N_\mathrm{t}\sum_{k'=1}^{N_\mathrm{s}-1}\gamma_{k'} + \sigma^2} \tag{12}$$

where $\gamma_{k'}$ was given in (10).

IV. Phase Noise Suppression and Data Detection

As mentioned in Section III, (1) and (2) do not hold for MIMO-OFDM systems in the presence of phase noise and time-selective fading. From (5), we have

$$\sum_{n=0}^{N_\mathrm{s}-1}\{\boldsymbol{H}_l(n)\}_{ij}\, e^{j\phi(n)} = \{\boldsymbol{H}_l(0)\}_{ij}\sum_{m=0}^{N_\mathrm{s}-1}\alpha_m e^{j\phi(m)} + \sum_{n=1}^{N_\mathrm{s}-1}\rho_{l,ij}(n)e^{j\phi(n)}. \tag{13}$$

Hence

$$\begin{aligned}\{\boldsymbol{G}_{kk}\}_{ij} &= \sum_{l=0}^{L-1}\sum_{n=0}^{N_\mathrm{s}-1} u_{kn}u^*_{k,[n-l]}\{\boldsymbol{H}_l(n)\}_{ij}\, e^{j\phi(n)} \\ &= \frac{1}{N_\mathrm{s}}\sum_{l=0}^{L-1} e^{-j\frac{2\pi}{N_\mathrm{s}}kl}\sum_{n=0}^{N_\mathrm{s}-1}\{\boldsymbol{H}_l(n)\}_{ij}\, e^{j\phi(n)} \\ &= \frac{1}{N_\mathrm{s}}\sum_{l=0}^{L-1} e^{-j\frac{2\pi}{N_\mathrm{s}}kl}\{\boldsymbol{H}_l(0)\}_{ij}\sum_{m=0}^{N_\mathrm{s}-1}\alpha_m e^{j\phi(m)} \\ &\quad + \frac{1}{N_\mathrm{s}}\sum_{l=0}^{L-1} e^{-j\frac{2\pi}{N_\mathrm{s}}kl}\sum_{n=1}^{N_\mathrm{s}-1}\rho_{l,ij}(n)e^{j\phi(n)}\end{aligned} \tag{14}$$

where u_{kn} and $u^*_{k,[n-l]}$ are defined in Appendix A. Thus, (7) can be modified as

$$\boldsymbol{y}_k = \boldsymbol{C}_{kk}\boldsymbol{x}_k\frac{1}{N_\mathrm{s}}\sum_{m=0}^{N_\mathrm{s}-1}\alpha_m e^{j\phi(m)} + \boldsymbol{P}_{kk}\boldsymbol{x}_k + \sum_{\substack{k'=0 \\ k' \neq k}}^{N_\mathrm{s}-1}\boldsymbol{G}_{kk'}\boldsymbol{x}_{k'} + \boldsymbol{n}_k \tag{15}$$

where $\{\boldsymbol{C}_{kk}\}_{ij} = \sum_{l=0}^{L-1} e^{-j(2\pi/N_\mathrm{s})kl}\{\boldsymbol{H}_l(0)\}_{ij}$ and $\{\boldsymbol{P}_{kk}\}_{ij} = (1/N_\mathrm{s})\sum_{l=0}^{L-1} e^{-j(2\pi/N_\mathrm{s})kl}\sum_{n=1}^{N_\mathrm{s}-1}\rho_{l,ij}(n)e^{j\phi(n)}$. Note that $(1/N_\mathrm{s})\sum_{m=0}^{N_\mathrm{s}-1}\alpha_m e^{j\phi(m)}$ in (15) is similar to $I(0)$ in (2), which is the CPE term. The term $\boldsymbol{P}_{kk}\boldsymbol{x}_k$ carries data symbols, but the

$$\mathrm{CIR} = \frac{N_\mathrm{s} + 2\sum_{i=1}^{N_\mathrm{s}-1}(N_\mathrm{s}-i)J_0(2\pi i f_\mathrm{d}T_\mathrm{s})e^{-\pi\beta T_\mathrm{s} i}}{\sum_{k'=1}^{N_\mathrm{s}-1}\left\{N_\mathrm{s} + 2\sum_{i=1}^{N_\mathrm{s}-1}(N_\mathrm{s}-i)J_0(2\pi i f_\mathrm{d}T_\mathrm{s})\cos\left(\frac{2\pi}{N_\mathrm{s}}k'i\right)e^{-\pi\beta T_\mathrm{s} i}\right\}} \tag{11}$$

distortion $\boldsymbol{P}_{kk}$ is a function of the phase noise process, which is costly to estimate. Additionally, when $N_{\rm s}$ is large, this term is very small due to the scaling factor $1/N_{\rm s}$. Therefore, the term $\boldsymbol{P}_{kk}\boldsymbol{x}_k$ will be treated as noise for the derivation of mmse-based phase noise mitigation and the third term on the right-hand side of (15) is the ICI term caused by both phase noise and time-selective fading.

For OFDM systems over fast-fading channels, channel estimates are generally obtained by transmitting pilot symbols at certain positions of the frequency-time grid [6], [22]–[24]. When significant phase noise is also present, a joint scheme to simultaneously estimate CPE and CSI is needed. Such a joint estimation appears to be very challenging because of the mutual coupling effects of phase-noise and channel fading processes as seen from (15), and is out of the scope of this paper. We thus assume perfect CSI in the receiver, but unknown CPE to make the analytical derivation tractable. Therefore, the CPE term $C(0) = (1/N_{\rm s})\sum_{m=0}^{N_{\rm s}-1}\alpha_m e^{j\phi(m)}$ must be estimated. In the following discussion, pilot signals are transmitted to estimate CPE. We rewrite (15) as

$$\boldsymbol{y}_{k\in N_p} = \boldsymbol{s}_{k\in N_p}C(0) + \boldsymbol{e}_{k\in N_p} \tag{16}$$

where $\boldsymbol{s}_k = \boldsymbol{C}_{kk}\boldsymbol{x}_k$, $\boldsymbol{e}_k = \boldsymbol{P}_{kk}\boldsymbol{x}_k + \sum_{k'=0,k'\neq k}^{N_{\rm s}-1}\boldsymbol{G}_{kk'}\boldsymbol{x}_{k'} + \boldsymbol{n}_k$, and N_p stands for the set of pilot signals, which will be omitted in the analysis of mmse for simplicity of notation. Let $\acute{\boldsymbol{N}}_k = E[\boldsymbol{e}_k\boldsymbol{e}_k^{\rm H}]$. As shown in Appendix C, $\acute{\boldsymbol{N}}_k$ can be expressed as

$$\begin{aligned}\acute{\boldsymbol{N}}_k &= E\left[\boldsymbol{e}_k\boldsymbol{e}_k^{\rm H}\right] \\ &= \left\{\frac{N_{\rm t}}{N_{\rm s}^2}\sum_{l=0}^{L-1}e^{-\frac{\tau_l}{\tau_{\rm rms}}}\sum_{n=1}^{N_{\rm s}-1}\left(1-J_0^2(2\pi n f_{\rm d}T_{\rm s})\right)\right. \\ &\qquad \left. + N_{\rm t}\sum_{k'=1}^{N_{\rm s}-1}\gamma_{k'} + \sigma^2\right\}\boldsymbol{I}_{N_{\rm r}}.\end{aligned} \tag{17}$$

The results given in (16) and (17) allow us to estimate the CPE term. When an mmse scheme is applied, the cost function $E[\|C(0) - \acute{\boldsymbol{W}}_k^{\rm H}\boldsymbol{y}_k\|_F^2]$ is minimized by finding an appropriate coefficient matrix $\acute{\boldsymbol{W}}_k$. With some algebraic manipulations, the optimal matrix in the mmse sense is determined to be

$$\acute{\boldsymbol{W}}_k = \left(\boldsymbol{s}_k\boldsymbol{s}_k^{\rm H} + \acute{\boldsymbol{N}}_k\right)^{-1}\boldsymbol{s}_k. \tag{18}$$

Thus, the mmse estimate of CPE is given by

$$\hat{C}(0) = \acute{\boldsymbol{W}}_k^{\rm H}\boldsymbol{y}_k = \boldsymbol{s}_k^{\rm H}\left(\boldsymbol{s}_k\boldsymbol{s}_k^{\rm H} + \acute{\boldsymbol{N}}_k\right)^{-1}\boldsymbol{y}_k. \tag{19}$$

CPE is the same for each subcarrier within one OFDM symbol. The effects of phase noise, time-selective fading, and the channel delay spread are jointly minimized through a single parameter $\hat{C}(0)$, which is a function of $\{\beta T_{\rm s}, f_{\rm d}T_{\rm s}, \tau_{\rm rms}, N_{\rm s}, N_{\rm t}, \sigma\}$. In what follows, we analyze a few existing detection schemes which incorporate the mmse estimate of CPE derived in this paper, that is, $\hat{C}(0)$ given in (19).

From the analysis above, we can relate the transmitted signals and received signals of the kth subcarrier as

$$\boldsymbol{y}_k = \boldsymbol{C}_{kk}\hat{C}(0)\boldsymbol{x}_k + \boldsymbol{e}_k. \tag{20}$$

When a simple ZF detection scheme is applied, $\boldsymbol{y}_k$ is processed as

$$\boldsymbol{\Theta}_k\boldsymbol{y}_k\hat{C}^{-1}(0) = \boldsymbol{\Theta}_k\boldsymbol{C}_{kk}\boldsymbol{x}_k + \boldsymbol{\Theta}_k\boldsymbol{e}_k\hat{C}^{-1}(0) \tag{21}$$

where $\Theta_k = \boldsymbol{C}_{kk}^{\dagger}$. Note that when $N_{\rm r} \geq N_{\rm t}$ and a linear detection scheme is adopted, a diversity order of $N_{\rm r} - N_{\rm t} + 1$ can be achieved. Based on (21), the least-square (LS) criterion can be used to detect the transmitted signal as

$$\hat{x}_{kp} = \underbrace{\operatorname{argmin}}_{x(i)\in\mathcal{A}}\left|[\boldsymbol{\Theta}_k]_p\boldsymbol{y}_k\hat{C}^{-1}(0) - x(i)\right|^2, \qquad p = 1,\ldots,N_{\rm t} \tag{22}$$

where $\mathcal{A}$ is the symbol alphabet and $[\Theta_k]_p$ is the pth row of Θ_k.

When the mmse detection scheme is considered, $E[\|\boldsymbol{x}_k - \acute{\boldsymbol{M}}_k^{\rm H}\boldsymbol{y}_k\|_F^2]$ is minimized by finding an matrix $\acute{\boldsymbol{M}}_k$, which is easily obtained as

$$\acute{\boldsymbol{M}}_k = \left(\boldsymbol{C}_{kk}\boldsymbol{C}_{kk}^{\rm H}\left|\hat{C}(0)\right|^2 + \acute{\boldsymbol{N}}_k\right)^{-1}\boldsymbol{C}_{kk}\hat{C}(0) \tag{23}$$

where $\acute{\boldsymbol{N}}_k$ was given in (17). Thus, the mmse criterion yields

$$\begin{aligned}\hat{\boldsymbol{x}}_k &= \acute{\boldsymbol{M}}_k^{\rm H}\boldsymbol{y}_k \\ &= \boldsymbol{C}_{kk}^{\rm H}\hat{C}^*(0)\left(\boldsymbol{C}_{kk}\boldsymbol{C}_{kk}^{\rm H}\left|\hat{C}(0)\right|^2 + \acute{\boldsymbol{N}}_k\right)^{-1}\boldsymbol{y}_k.\end{aligned} \tag{24}$$

The decorrelating DF and the mmse-DF schemes have been shown to provide better performance than the ZF and the mmse schemes [25]. In the decorrelating DF detection, $\boldsymbol{y}_k$ is premultiplied by $\mathcal{L}^{-1}\boldsymbol{C}_{kk}^{\rm H}\hat{C}^{-1}(0)$ as

$$\begin{aligned}\widetilde{\boldsymbol{y}}_k &= \mathcal{L}^{-1}\boldsymbol{C}_{kk}^{\rm H}\hat{C}^{-1}(0)\boldsymbol{y}_k \\ &= \mathcal{L}^{-1}\boldsymbol{C}_{kk}^{\rm H}\boldsymbol{C}_{kk}\boldsymbol{x}_k + \mathcal{L}^{-1}\boldsymbol{C}_{kk}^{\rm H}\hat{C}^{-1}(0)\boldsymbol{e}_k \\ &= \mathcal{L}^{\rm H}\boldsymbol{x}_k + \boldsymbol{d}_k\end{aligned} \tag{25}$$

where $\mathcal{L}^{\rm H}$ is an upper triangular matrix obtained by using the Cholesky decomposition as

$$\mathcal{R} = \boldsymbol{C}_{kk}^{\rm H}\boldsymbol{C}_{kk} = \mathcal{L}\mathcal{L}^{\rm H}.$$

The pth component of $\widetilde{\boldsymbol{y}}_k$ is given by

$$\widetilde{y}_{kp} = \{\mathcal{L}^{\rm H}\}_{pp}x_{kp} + \sum_{i=p+1}^{N_{\rm t}}\{\mathcal{L}^{\rm H}\}_{pi}x_{ki} + d_{kp}. \tag{26}$$

Finally, the transmitted symbols are detected as

$$\begin{aligned}\hat{x}_{kN_{\rm t}} &= \operatorname{dec}\left(\widetilde{y}_{kN_{\rm t}}\right) \\ \hat{x}_{kp} &= \operatorname{dec}\left(\widetilde{y}_{kp} - \sum_{i=p+1}^{N_{\rm t}}\{\mathcal{L}^{\rm H}\}_{pi}\hat{x}_{ki}\right), \qquad p = 1,\ldots,N_{\rm t}-1\end{aligned}$$

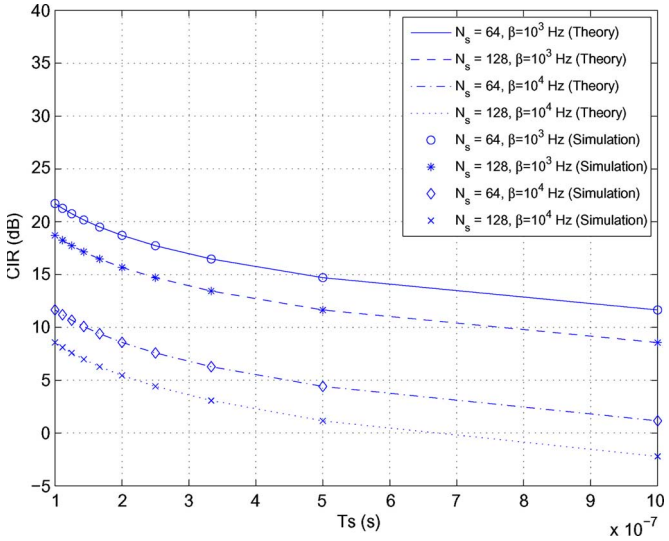

Fig. 1. CIR comparisons with different number of subcarriers and phase noise linewidth ($v_s = 100$ km/h).

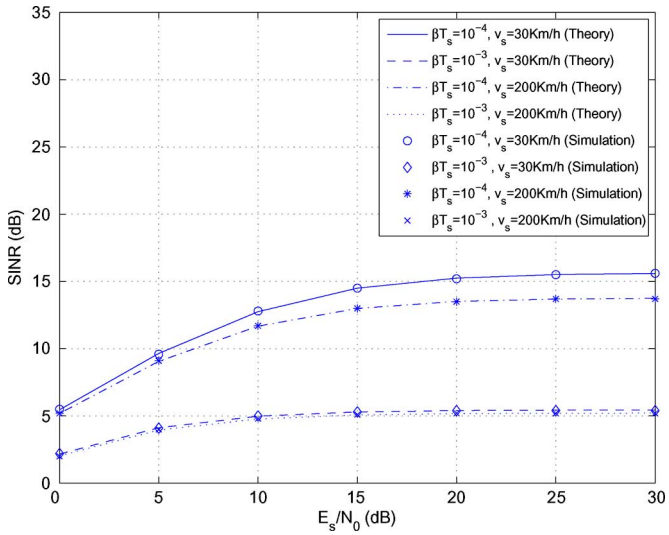

Fig. 2. SINR versus E_s/N_0 for MIMO-OFDM with different vehicle speed and phase noise variance ($N_s = 256$, $T_s = 10^{-6}$ s).

where $\mathrm{dec}(\cdot)$ is the slice function corresponding to the specific modulation applied. The mmse-DF scheme is the one that minimizes the average energy of $\widetilde{y}_{kp} - x_{kp}$, $p = 1, \ldots, N_t$, under the assumption that previously detected signals in the feedback filter are correct. Details of this scheme can be found in [16], [17] and [26].

V. Simulation Results and Discussion

Simulations are carried out based on the "SUI-5" channel model [27], which is one of six channel models adopted by IEEE 802.16a for evaluating broadband wireless systems in the 2–11-GHz band. We consider a system with two transmit antennas and three receive antennas which employs quaternary phase-shift keying (QPSK) modulation. The doubly selective Rayleigh fading channel is assumed to have three resolvable multipath components. These paths are modeled as independent complex Gaussian random variables and have relative delays of 0, 5, and 10 μs. The rms delay spread of the channel is 3.05 μs and the maximum Doppler shift of the channel is calculated based on a carrier frequency of $f_c = 2$ GHz.

Fig. 1 shows the CIR values as a function of data symbol period T_s, the 3-dB phase noise linewidth β, and the number of subcarriers N_s within one OFDM symbol. These curves are obtained by using the analytical expression given in (11) and simulations based on the maximum Doppler shift under a vehicle speed of $v_s = 100$ km/h. Simulation results match well with the theoretical results. CIR is found to be inversely proportional to T_s, N_s, and β; thus, increasing β or T_s makes the MIMO-OFDM system more vulnerable to phase noise or time variations of the channel coefficients.

In Fig. 2, SINR versus E_s/N_0 curves under different values of βT_s and v_s are obtained by using (12) and computer simulations. The OFDM symbol is assumed to have $N_s = 256$ subcarriers, and data symbol period is $T_s = 10^{-6}$ s. It is observed that SINR is inversely proportional to βT_s. With a fixed but large value of βT_s (e.g., 10^{-3}), however, the difference between SINR curves corresponding to different vehicle speeds

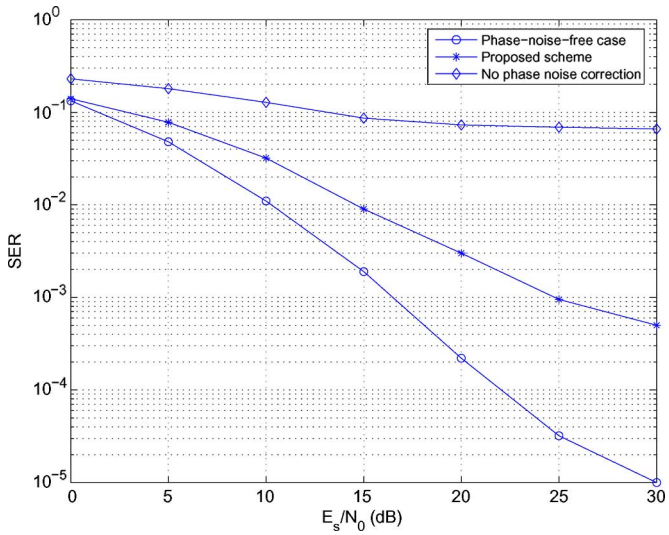

Fig. 3. SER versus E_s/N_0 for MIMO-OFDM with phase noise $\beta T_s = 10^{-6}$ ($N_s = 128$, $T_s = 10^{-7}$ s, $v_s = 30$ km/h).

diminishes. This is because when βT_s is large, ICI is dominated by phase noise. On the other hand, with a smaller βT_s value such as $\beta T_s = 10^{-4}$, increasing the Doppler shift (or vehicle speed) clearly lowers the SINR value.

Fig. 3 shows the SER performance of the proposed mmse-based phase noise suppression scheme, together with those of a phase-noise-free system, and a system without phase noise correction when the mmse detection scheme given by (24) is considered. System parameters chosen are the following: $N_s = 128$, $T_s = 10^{-7}$ s, $\beta = 10$ Hz, and $v_s = 30$ km/h. It is observed that without phase noise correction, even a very mild amount of phase noise ($\beta T_s = 10^{-6}$) causes a high error floor. On the other hand, the proposed scheme significantly reduces the effect of phase noise. Note that performance of the proposed scheme does not approach that of the phase-noise-free system because this scheme mitigates only CPE, and it does not eliminate ICI, which is caused by both phase noise and time-selective fading.

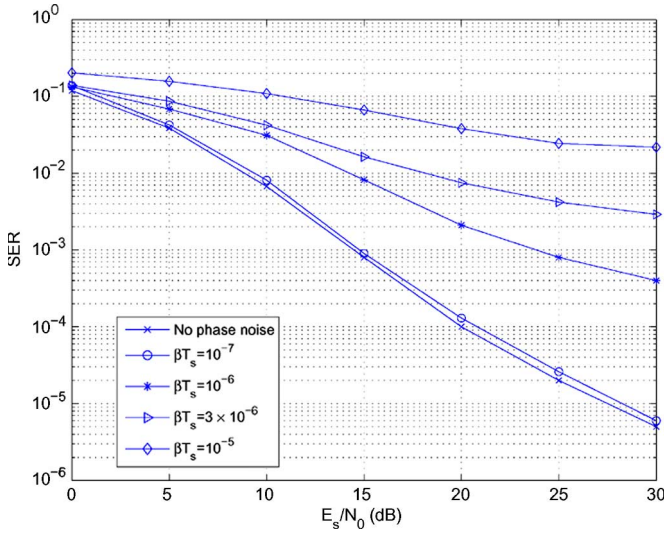

Fig. 4. SER versus E_s/N_0 for MIMO-OFDM with different phase noise variance ($N_s = 64$, $T_s = 10^{-7}$ s, $v_s = 100$ km/h).

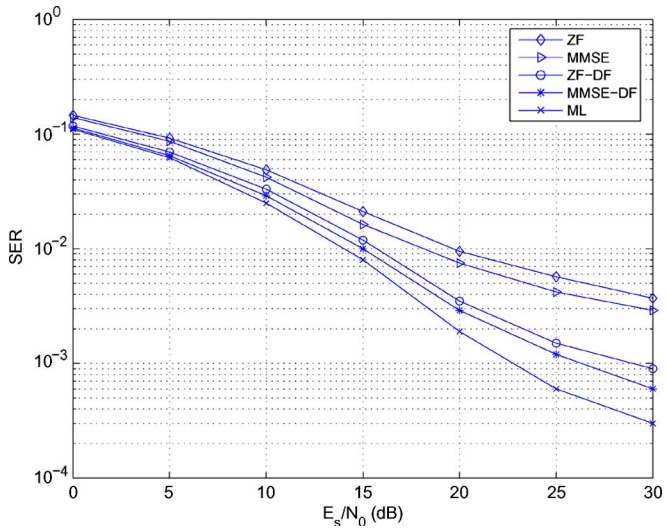

Fig. 5. SER versus E_s/N_0 for MIMO-OFDM with different detection schemes ($\beta T_s = 3 \times 10^{-6}$, $N_s = 64$, $v_s = 100$ km/h).

Shown in Fig. 4 are the simulated SER performances of the system when the proposed mmse-based phase noise suppression scheme given by (19) and the mmse detection scheme described by (24) are employed. Other parameters chosen are the following: $N_s = 64$, $T_s = 10^{-7}$ s, and $v_s = 100$ km/h. Performances with different values of the 3-dB phase noise variance ($\beta T_s = 10^{-7}, 10^{-6}, 3 \times 10^{-6}$, and 10^{-5}) are compared. The performance curve of a phase-noise-free MIMO-OFDM system is used as the baseline performance. It appears that the scheme works effectively only when βT_s is small.

In Fig. 5, we compare the performances of four different detection methods: the ZF, mmse, decorrelating DF (also known as the ZF–DF), and mmse-DF schemes when the mmse-based phase noise suppression scheme given by (19) is applied. Other than that $\beta = 30$ Hz, all other parameters are the same as those applied for Fig. 4. Performance of the maximum-likelihood scheme is used as the benchmark for other detection schemes. Since these schemes are not specifically optimized for MIMO-OFDM systems with phase noise over fast time-varying fading channels for which ICI should be dealt with, error floors are observed for all cases. Note that from (10) and (11), the energy of ICI due to the phase noise and time-selective fading is found to spread over all subcarriers, which is different from the assumption in [28] that most of ICI on each subcarrier comes from several neighboring subcarriers. Consequently, ICI suppression for the scenario studied in this paper becomes more challenging than the case dealt with in [28].

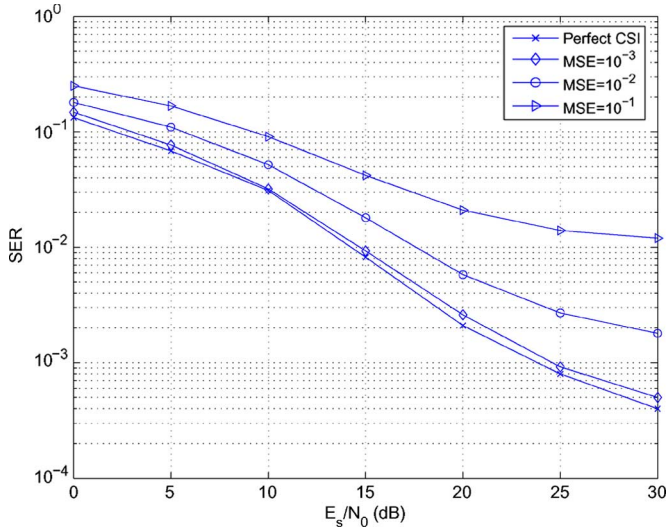

Fig. 6. SER versus E_s/N_0 for MIMO-OFDM with different mse ($\beta T_s = 10^{-6}$, $N_s = 64$, $v_s = 100$ km/h).

We have assumed perfect CSI for all numerical results so far. In practical systems, however, there exist channel estimation errors. It is beyond the scope of this paper to discuss channel estimation schemes for time-selective fading channels. To access its impact, channel estimation error is emulated by introducing an error with a normalized average mean square error (mse) defined as mse $= E[\|\hat{\breve{\boldsymbol{H}}} - \breve{\boldsymbol{H}}\|_F^2]/E[\|\breve{\boldsymbol{H}}\|_F^2]$, where $\breve{\boldsymbol{H}}$ has the same form as (4), except that phase noise terms and OFDM symbol index are neglected. The performance results of MIMO-OFDM systems with various mse values are shown in Fig. 6, where all parameters, except $\beta = 10$ Hz, are the same as those applied in Fig. 5. The proposed mmse-based phase-noise suppression scheme and the mmse detection scheme are employed in this simulation. It is observed that the performance degradation is negligible only when the mse value of channel estimation errors is small (e.g., 10^{-3}).

VI. Conclusion

We have analyzed the impact of phase noise and channel time selectivity on the performance of MIMO-OFDM systems. Specifically, we have quantified ICI caused by phase noise and channel time-variations. A phase noise suppression scheme based on the minimum mean-square-error criterion is proposed, which is shown to effectively reduce the effect of phase noise. Performances of four detection schemes are compared, and it seems that none of them can effectively eliminate the error floor of MIMO-OFDM systems in the presence of phase noise and doubly selective fading. It is also observed that an increase

in the 3-dB phase noise linewidth, the data symbol period, or the number of OFDM subcarriers lowers the achievable carrier-to-interference power ratio. Moreover, it is found that an increase in channel estimation error could deteriorate the system performance dramatically.

APPENDIX A
PROOF THAT $\boldsymbol{\Upsilon}$ IS A CIRCULANT MATRIX AND DERIVATION OF (10)

Since $\boldsymbol{\Upsilon}$ with dimension $N_\mathrm{s} \times N_\mathrm{s}$ in (8) is the same for any antenna index (i, j), we can replace matrix $\boldsymbol{H}_l(n)$ of the channel matrix $\boldsymbol{H}$ in (4) with a scalar $h_l(n)$ (note that OFDM symbol index is omitted for notational simplicity) and replace the zero matrix $\mathbf{0}$ with a scalar 0, forming a new $N_\mathrm{s} \times N_\mathrm{s}$ matrix $\mathcal{H}$. If we denote $\mathcal{H}$ as the sum of L matrices as $\mathcal{H} = \sum_{l=0}^{L-1} \mathcal{H}_{(l)}$, where $\mathcal{H}_{(l)}$ is a matrix formed by cyclically left-shifting the diagonal matrix $\mathrm{diag}\{h_l(0)e^{j\phi(0)}, \ldots, h_l(N_\mathrm{s}-1)e^{j\phi(N_\mathrm{s}-1)}\}$ by l columns, we have

$$\mathcal{G} = U\mathcal{H}U^\mathrm{H} = \sum_{l=0}^{L-1} \mathcal{G}_l = \sum_{l=0}^{L-1} U\mathcal{H}_{(l)}U^\mathrm{H} \tag{27}$$

where $\boldsymbol{U} = [\boldsymbol{u}_0, \ldots, \boldsymbol{u}_{N_\mathrm{s}-1}]$ is the unitary DFT matrix. With the conditions that

$$\begin{aligned}
&E\left[h_l(n)e^{j\phi(n)}\right] \\
&\quad = 0, \qquad l = 0, \ldots, L-1; \quad n = 0, \ldots, N_\mathrm{s}-1 \\
&E\left[h_l(r)e^{j\phi(r)} \cdot h_{l'}^*(s)e^{-j\phi(s)}\right] \\
&\quad = E\left[h_l(r) \cdot h_{l'}^*(s)\right] E\left[e^{j\phi(r)} \cdot e^{-j\phi(s)}\right] \\
&\quad = J_0(2\pi|r-s|f_\mathrm{d}T_\mathrm{s})\delta_{l-l'}e^{-\frac{\tau_l}{\tau_\mathrm{rms}}-|r-s|\pi\beta T_\mathrm{s}}, \\
&\qquad r, s = 0, \ldots, N_\mathrm{s}-1
\end{aligned} \tag{28}$$

it is recognized that $\boldsymbol{\Upsilon} = \sum_{l=0}^{L-1} \boldsymbol{\Upsilon}_l$, where $\boldsymbol{\Upsilon}_l$ is an $N_\mathrm{s} \times N_\mathrm{s}$ matrix and $\{\boldsymbol{\Upsilon}_l\}_{ij} = \mathrm{var}(\{\mathcal{G}_l\}_{ij})$. Since the sum of circulant matrices of the same dimension is also a circulant matrix, we only need to prove that each $\boldsymbol{\Upsilon}_l$ is a circulant matrix.

For any integer n, let $[n]$ denote n modulo N_s, i.e., $[n]$ is the remainder from dividing n by N_s. The $\{\mathcal{G}_l\}_{ij}$ is obtained as

$$\{\mathcal{G}_l\}_{ij} = \boldsymbol{u}_i^\mathrm{T}\mathcal{H}_{(l)}\boldsymbol{u}_j^* = \boldsymbol{\eta}_{ij}^\mathrm{T}\boldsymbol{h}_l \tag{29}$$

where $\boldsymbol{\eta}_{ij} = [\eta_{ij0}, \ldots, \eta_{ij,(N_\mathrm{s}-1)}]^\mathrm{T}$, $\boldsymbol{u}_i = [u_{i0}, \ldots, u_{i,(N_\mathrm{s}-1)}]^\mathrm{T}$, $\eta_{ijn} = u_{in}u_{j,[n-l]}^*$, and $\boldsymbol{h}_l = [h_l(0)e^{j\phi(0)}, \ldots, h_l(N_\mathrm{s}-1)e^{j\phi(N_\mathrm{s}-1)}]^\mathrm{T}$. Thus

$$\begin{aligned}
\{\boldsymbol{\Upsilon}_l\}_{ij} &= \mathrm{var}(\boldsymbol{\eta}_{ij}^\mathrm{T}\boldsymbol{h}_l) \\
&= \sum_{r=0}^{N_\mathrm{s}-1}\sum_{s=0}^{N_\mathrm{s}-1} \eta_{ijr}\chi(r,s)\eta_{ijs}^* \\
&= \frac{1}{N_\mathrm{s}^2}\sum_{r=0}^{N_\mathrm{s}-1}\sum_{s=0}^{N_\mathrm{s}-1} \chi(r,s)e^{-(2\pi\sqrt{-1}/N_\mathrm{s})t_{ijrs}}
\end{aligned} \tag{30}$$

where $\chi(r,s) = \mathrm{cov}(h_l(r)e^{j\phi(r)} \cdot h_l^*(s)e^{-j\phi(s)})$ and $t_{ijrs} = ir - j[r-l] - is + j[s-l]$. It suffices to show, for any fixed r and s, that $[t_{ijrs}] = [ir - j[r-l] - is + j[s-l]] = [j-i][s-r]$. Also note that an $N_\mathrm{s} \times N_\mathrm{s}$ matrix $\boldsymbol{B}$ is circulant if and only if $\{\boldsymbol{B}\}_{ij} = \kappa_{[j-i]}$, i.e., if and only if $\{\boldsymbol{B}\}_{ij}$ depends only on $[j-i]$ and $e^{-(2\pi\sqrt{-1}/N_\mathrm{s})k} = e^{-(2\pi\sqrt{-1}/N_\mathrm{s})[k]}$ because $e^{2\pi\sqrt{-1}} = 1$. Thus, from (30), we can conclude that $\boldsymbol{\Upsilon}_l$ is a circulant matrix if $h_l(n)$, $n = 0, \ldots, N_\mathrm{s}-1$, are finite.

Moreover, from (30), we have

$$\begin{aligned}
\{\boldsymbol{\Upsilon}\}_{ij} &= \sum_{l=0}^{L-1}\{\boldsymbol{\Upsilon}_l\}_{ij} \\
&= \frac{1}{N_\mathrm{s}^2}\sum_{l=0}^{L-1}\sum_{r=0}^{N_\mathrm{s}-1}\sum_{s=0}^{N_\mathrm{s}-1} J_0(2\pi|r-s|f_\mathrm{d}T_\mathrm{s}) \\
&\qquad \times e^{-(2\pi\sqrt{-1}/N_\mathrm{s})t_{ijrs}}e^{-\frac{\tau_l}{\tau_\mathrm{rms}}-|r-s|\pi\beta T_\mathrm{s}} \\
&= \frac{1}{N_\mathrm{s}^2}\sum_{l=0}^{L-1}\left\{N_\mathrm{s} + 2\sum_{m=1}^{N_\mathrm{s}-1}(N_\mathrm{s}-m)J_0(2\pi m f_\mathrm{d}T_\mathrm{s})\right. \\
&\qquad \left. \times \cos\left(\frac{2\pi}{N_\mathrm{s}}[j-i]m\right)e^{-\pi\beta T_\mathrm{s}m}\right\}e^{-\frac{\tau_l}{\tau_\mathrm{rms}}}
\end{aligned} \tag{31}$$

APPENDIX B
DERIVATIONS OF (11) AND (12)

The derivation of (11) is given by (32) and (33), shown at the top of the next page.

APPENDIX C
DERIVATION OF (17)

From the assumptions made in (5), it is clear that $\rho_{l,ij}(n)$ are independent Gaussian random variables with $E[\rho_{l,ij}(n)\rho_{l',i'j'}^*(n')] = e^{-(\tau_l/\tau_\mathrm{rms})}(1-J_0^2(2\pi n f_\mathrm{d}T_\mathrm{s}))\delta_{l-l'}\delta_{i-i'}\delta_{j-j'}\delta_{n-n'}$. With some simple manipulations, we have

$$\begin{aligned}
&E\left[(\boldsymbol{P}_{kk}\boldsymbol{x}_k)(\boldsymbol{P}_{kk}\boldsymbol{x}_k)^\mathrm{H}\right] \\
&\quad = E\left[\boldsymbol{P}_{kk}\boldsymbol{P}_{kk}^\mathrm{H}\right] \\
&\quad = \left\{\frac{N_\mathrm{t}}{N_\mathrm{s}^2}\sum_{l=0}^{L-1}e^{-\frac{\tau_l}{\tau_\mathrm{rms}}}\sum_{n=1}^{N_\mathrm{s}-1}\left(1 - J_0^2(2\pi n f_\mathrm{d}T_\mathrm{s})\right)\right\}\boldsymbol{I}_{N_\mathrm{r}}.
\end{aligned} \tag{34}$$

Together with $E[\{\boldsymbol{H}_l(n)\}_{ij}\{\boldsymbol{H}_l(n)\}_{i'j'}^*] = e^{-(\tau_l/\tau_\mathrm{rms})}\delta_{i-i'}\delta_{j-j'}$, we have $E[\{\boldsymbol{G}_{kk'}\}_{ij}\{\boldsymbol{G}_{kk'}\}_{i'j'}^*] = 0$, $i \neq i'$ or $j \neq j'$, because $\{\boldsymbol{G}_{kk'}\}_{ij} = \sum_{l=0}^{L-1}\sum_{n=0}^{N_\mathrm{s}-1} u_{kn}u_{k',[n-l]}^*\{\boldsymbol{H}_l(n)\}_{ij}e^{j\phi(n)}$. Thus, we obtain

$$\begin{aligned}
&E\left[\left(\sum_{\substack{k'=0\\k'\neq k}}^{N_\mathrm{s}-1}\boldsymbol{G}_{kk'}\boldsymbol{x}_{k'}\right)\left(\sum_{\substack{k'=0\\k'\neq k}}^{N_\mathrm{s}-1}\boldsymbol{G}_{kk'}\boldsymbol{x}_{k'}\right)^\mathrm{H}\right] \\
&\quad = \sum_{\substack{k'=0\\k'\neq k}}^{N_\mathrm{s}-1}E\left[\boldsymbol{G}_{kk'}\boldsymbol{G}_{kk'}^\mathrm{H}\right] \\
&\quad = \left(N_\mathrm{t}\sum_{k'=1}^{N_\mathrm{s}-1}\gamma k'\right)\boldsymbol{I}_{N_\mathrm{r}}.
\end{aligned} \tag{35}$$

$$
\begin{aligned}
\mathrm{CIR} &= \frac{E\left[\|\boldsymbol{G}_{kk}\boldsymbol{x}_k\|_F^2\right]}{E\left[\left\|\sum\limits_{\substack{k'=0\\k'\neq k}}^{N_\mathrm{s}-1}\boldsymbol{G}_{kk'}\boldsymbol{x}_{k'}\right\|_F^2\right]} \\
&= \frac{\mathrm{tr}\left\{E\left[\boldsymbol{G}_{kk}\boldsymbol{x}_k\boldsymbol{x}_k^{\mathrm{H}}\boldsymbol{G}_{kk}^{\mathrm{H}}\right]\right\}}{\mathrm{tr}\left\{E\left[\left(\sum\limits_{\substack{k'=0\\k'\neq k}}^{N_\mathrm{s}-1}\boldsymbol{G}_{kk'}\boldsymbol{x}_{k'}\right)\left(\sum\limits_{\substack{k'=0\\k'\neq k}}^{N_\mathrm{s}-1}\boldsymbol{G}_{kk'}\boldsymbol{x}_{k'}\right)^{\mathrm{H}}\right]\right\}} \\
&= \frac{\gamma_0}{\sum\limits_{k'=1}^{N_\mathrm{s}-1}\gamma k'} \\
&= \frac{\sum\limits_{l=0}^{L-1}\left\{N_\mathrm{s}+2\sum\limits_{i=1}^{N_\mathrm{s}-1}(N_\mathrm{s}-i)\alpha_i e^{-\pi\beta T_\mathrm{s} i}\right\}e^{-\frac{\tau_l}{\tau_{\mathrm{rms}}}}}{\sum\limits_{k'=1}^{N_\mathrm{s}-1}\sum\limits_{l=0}^{L-1}\left\{N_\mathrm{s}+2\sum\limits_{i=1}^{N_\mathrm{s}-1}(N_\mathrm{s}-i)\alpha_i\cos\left(\frac{2\pi}{N_\mathrm{s}}k'i\right)e^{-\pi\beta T_\mathrm{s} i}\right\}e^{-\frac{\tau_l}{\tau_{\mathrm{rms}}}}} \\
&= \frac{N_\mathrm{s}+2\sum\limits_{i=1}^{N_\mathrm{s}-1}(N_\mathrm{s}-i)J_0(2\pi i f_\mathrm{d}T_\mathrm{s})e^{-\pi\beta T_\mathrm{s} i}}{\sum\limits_{k'=1}^{N_\mathrm{s}-1}\left\{N_\mathrm{s}+2\sum\limits_{i=1}^{N_\mathrm{s}-1}(N_\mathrm{s}-i)J_0(2\pi i f_\mathrm{d}T_\mathrm{s})\cos\left(\frac{2\pi}{N_\mathrm{s}}k'i\right)e^{-\pi\beta T_\mathrm{s} i}\right\}}
\end{aligned}
\tag{32}
$$

$$
\begin{aligned}
\mathrm{SINR} &= \frac{E\left[\|\boldsymbol{G}_{kk}\boldsymbol{x}_k\|_F^2\right]}{E\left[\left\|\sum\limits_{\substack{k'=0\\k'\neq k}}^{N_\mathrm{s}-1}\boldsymbol{G}_{kk'}\boldsymbol{x}_{k'}+\boldsymbol{n}_k\right\|_F^2\right]} \\
&= \frac{\mathrm{tr}\left\{E\left[\boldsymbol{G}_{kk}\boldsymbol{x}_k\boldsymbol{x}_k^{\mathrm{H}}\boldsymbol{G}_{kk}^{\mathrm{H}}\right]\right\}}{\mathrm{tr}\left\{E\left[\left(\sum\limits_{\substack{k'=0\\k'\neq k}}^{N_\mathrm{s}-1}\boldsymbol{G}_{kk'}\boldsymbol{x}_{k'}\right)\left(\sum\limits_{\substack{k'=0\\k'\neq k}}^{N_\mathrm{s}-1}\boldsymbol{G}_{kk'}\boldsymbol{x}_{k'}\right)^{\mathrm{H}}+\boldsymbol{n}_k\boldsymbol{n}_k^{\mathrm{H}}\right]\right\}} \\
&= \frac{N_\mathrm{t}\gamma_0}{N_\mathrm{t}\sum\limits_{k'=1}^{N_\mathrm{s}-1}\gamma_{k'}+\sigma^2}
\end{aligned}
\tag{33}
$$

Since $E[\boldsymbol{n}_k\boldsymbol{n}_k^{\mathrm{H}}]=\sigma^2\boldsymbol{I}_{N_\mathrm{r}}$, we have

$$
\begin{aligned}
E\left[e_k e_k^H\right] &= E\left[\left(\boldsymbol{P}_{kk}\boldsymbol{x}_k+\sum_{\substack{k'=0\\k'\neq k}}^{N_\mathrm{s}-1}\boldsymbol{G}_{kk'}\boldsymbol{x}_{k'}+\boldsymbol{n}_k\right)\right. \\
&\qquad\left.\times\left(\boldsymbol{P}_{kk}\boldsymbol{x}_k+\sum_{\substack{k'=0\\k'\neq k}}^{N_\mathrm{s}-1}\boldsymbol{G}_{kk'}\boldsymbol{x}_{k'}+\boldsymbol{n}_k\right)^{\mathrm{H}}\right] \\
&= E\left[\boldsymbol{P}_{kk}\boldsymbol{P}_{kk}^{\mathrm{H}}\right]+\sum_{\substack{k'=0\\k'\neq k}}^{N_\mathrm{s}-1}E\left[\boldsymbol{G}_{kk'}\boldsymbol{G}_{kk'}^{\mathrm{H}}\right]+E\left[\boldsymbol{n}_k\boldsymbol{n}_k^{\mathrm{H}}\right] \\
&= \left\{\frac{N_\mathrm{t}}{N_\mathrm{s}^2}\sum_{l=0}^{L-1}e^{-\frac{\tau_l}{\tau_{\mathrm{rms}}}}\sum_{n=1}^{N_\mathrm{s}-1}\left(1-J_0^2(2\pi n f_\mathrm{d}T_\mathrm{s})\right)\right. \\
&\qquad\left.+N_\mathrm{t}\sum_{k'=1}^{N_\mathrm{s}-1}\gamma_{k'}+\sigma^2\right\}\boldsymbol{I}_{N_\mathrm{r}}.
\end{aligned}
\tag{36}
$$

REFERENCES

[1] T. Pollet, M. Bladel, and M. Moeneclaey, "BER sensitivity of OFDM systems to carrier frequency offset and Wiener phase noise," *IEEE Trans. Commun.*, vol. 43, no. 2/3/4, pp. 191–193, Feb./Mar./Apr. 1995.

[2] L. Tomba, "On the effect of Wiener phase noise in OFDM systems," *IEEE Trans. Commun.*, vol. 46, no. 5, pp. 580–583, May 1998.

[3] A. G. Armada, "Understanding the effects of phase noise in orthogonal frequency division multiplexing (OFDM)," *IEEE Trans. Broadcast*, vol. 47, no. 2, pp. 153–159, Jun. 2001.

[4] S. Wu and Y. Bar-Ness, "A phase noise suppression algorithm for OFDM based WLANs," *IEEE Commun. Lett.*, vol. 6, no. 12, pp. 535–537, Dec. 2002.

[5] G. Liu and W. Zhu, "Compensation of phase noise in OFDM systems using an ICI reduction scheme," *IEEE Trans. Broadcast*, vol. 50, no. 4, pp. 399–407, Dec. 2004.

[6] S. Wu and Y. Bar-Ness, "OFDM systems in the presence of phase noise: Consequences and solutions," *IEEE Trans. Commun.*, vol. 52, no. 11, pp. 1988–1996, Nov. 2004.

[7] G. J. Stüber, J. R. Barry, S. W. Mclaughlin, Y. Li, M. A. Ingram, and T. G. Pratt, "Broadband MIMO-OFDM wireless communications," *Proc. IEEE*, vol. 92, no. 2, pp. 271–294, Feb. 2004.

[8] T. C. W. Schnek, X.-J. Tao, P. F. M. Smulders, and E. R. Fledderus, "Influence and suppression of phase noise in multi-antenna OFDM," in *Proc. IEEE VTC—Fall*, Sep. 2004, pp. 1443–1447.

[9] K. Nikitopoulos and A. Polydoros, "Decision-directed compensation of phase noise and residual frequency offset in a space–time OFDM receiver," *IEEE Commun. Lett.*, vol. 8, no. 9, pp. 573–575, Sep. 2004.
[10] M. Russell and G. J. Stüber, "Interchannel interference analysis of OFDM in a mobile environment," in *Proc. IEEE Veh. Technol. Conf.*, 1995, pp. 820–824.
[11] J. Li and M. Kavehrad, "Effects of time selective multipath fading on OFDM systems for broadband mobile applications," *IEEE Commun. Lett.*, vol. 3, no. 12, pp. 332–334, Dec. 1999.
[12] A. Stamoulis, S. N. Diggavi, and N. Al-Dhahir, "Intercarrier interference in MIMO OFDM," *IEEE Trans. Signal Process.*, vol. 50, no. 10, pp. 2451–2464, Oct. 2002.
[13] S. Verdú, *Multiuser Detection*. Cambridge, U.K.: Cambridge Univ. Press, 1998.
[14] J. G. Proakis, *Digital Communications*, 4th ed. New York: McGraw-Hill, 2001.
[15] A. Duel-Hallen, "Decorrelating decision-feedback multiuser detector for synchronous code-division multiple-access channel," *IEEE Trans. Commun.*, vol. 41, no. 2, pp. 285–290, Feb. 1993.
[16] J. Cioffi, G. Dudevoir, M. Eyuboglu, and G. D. Forney, Jr., "MMSE decision-feedback equalizers and coding—Part I: Equalization results," *IEEE Trans. Commun.*, vol. 43, no. 10, pp. 2582–2694, Oct. 1995.
[17] J. Cioffi, G. Dudevoir, M. Eyuboglu, and G. D. Forney, Jr., "MMSE decision feedback equalization and coding—Part II: Coding results," *IEEE Trans. Commun.*, vol. 43, no. 10, pp. 2595–2604, Oct. 1995.
[18] Y. Zhang and H. Liu, "Frequency-domain correlative coding for MIMO-OFDM systems over fast fading channels," *IEEE Commun. Lett.*, vol. 10, no. 5, pp. 347–349, May 2006.
[19] O. Edfors, M. Sandell, J.-J. van der Beek, S. K. Wilson, and P. O. Börjesson, "OFDM channel estimation by singular value decomposition," *IEEE Trans. Commun.*, vol. 46, no. 7, pp. 931–939, Jul. 1998.
[20] F. C. Zheng and A. G. Burr, "Signal detection for non-orthogonal space-time block coding over time-selective fading channels," *IEEE Commun. Lett.*, vol. 8, no. 8, pp. 491–493, Aug. 2004.
[21] Y. Zhao and S. G. Häggman, "Intercarrier interference compression in OFDM communication systems by using correlative coding," *IEEE Commun. Lett.*, vol. 2, no. 8, pp. 214–216, Aug. 1998.
[22] S. Coleri, M. Ergen, and A. Bahai, "Channel estimation techniques based on pilot arrangement in OFDM systems," *IEEE Trans. Broadcast.*, vol. 48, no. 3, pp. 223–229, Sep. 2002.
[23] O. Simeone, Y. Bar-Ness, and U. Spagnolini, "Pilot-based channel estimation for OFDM systems by tracking the delay-subspace," *IEEE Trans. Wireless Commun.*, vol. 3, no. 1, pp. 315–325, Jan. 2004.
[24] S. Wu and Y. Bar-Ness, "A phase noise suppression algorithm for OFDM-based WLANs," *IEEE Commun. Lett.*, vol. 6, no. 12, pp. 535–537, Dec. 2002.
[25] Q. Meng, J. Zhang, and K. M. Wong, "Comparison of MBER transceiver designs for block data transmission," in *Proc. 22nd. Biennial Symp. Commun.*, Jun. 2004.
[26] A. Duel-Hallen, "Equalizers for multiple input/multiple output channels and PAM systems with cyclostationary input sequences," *IEEE J. Sel. Areas Commun.*, vol. 10, no. 3, pp. 630–639, Apr. 1992.
[27] D. Falconer, S. L. Ariyavisitakul, A. Benyamin-Seeyar, and B. Eidson, "Frequency domain equalization for single-carrier broadband wireless systems," *IEEE Commun. Mag.*, vol. 40, no. 4, pp. 58–66, Apr. 2002.
[28] X. Cai and G. B. Giannakis, "Bounding performance and suppressing intercarrier interference in wireless mobile OFDM," *IEEE Trans. Commun.*, vol. 51, no. 12, pp. 2047–2056, Dec. 2003.

Yu Zhang (S'05) received the B.E. and M.S. degrees in electronic engineering from Tsinghua University, Beijing, China, in 1999 and 2002, respectively, and is currently working toward the Ph.D. degree in electrical engineering and computer science at Oregon State University, Corvallis.

His current research interests include the performance analysis and detection schemes for multiple-input multiple-output orthogonal frequency division multiplexing systems over doubly selective fading channels, transmitter and receiver diversity techniques, and channel estimation and equalization algorithms.

Huaping Liu (S'95–M'97) received the B.S. and M.S. degrees from Nanjing University of Posts and Telecommunications, Nanjing, China, in 1987 and 1990, respectively, and the Ph.D. degree from the New Jersey Institute of Technology (NJIT), Newark, in 1997, all in electrical engineering.

From July 1997 to August 2001, he was with Lucent Technologies, NJ. He was with the School of Electrical Engineering and Computer Science, Oregon State University, Corvallis, in September 2001, where he is currently an Associate Professor. His research interests include capacity and performance analysis of wireless networks, communication techniques for multiuser time-varying environments with applications to cellular and indoor wireless communications, ultra-wideband schemes, and multiple-input multiple-output orthogonal frequency division multiplexing systems.